IOL Constant Optimization

36

Petros Aristodemou

Refinements in surgical technique, advances in biometry instrumentation, and the evolution of IOL power formulae have all brought about progressive improvements in predicting the refractive outcome following cataract surgery. Improving predictions depends on reducing random and systematic error, thus improving precision and accuracy, respectively.

Accuracy vs Precision

Random error refers to the degree of spread of the outcomes. The lower the random error, the tighter the spread, and the greater the precision. This is the difference of spread comparing the wide spread of hits using a regular gun (Target A) and the tight spread of hits using a sniper gun (targets B and C) (Table 36.1). Optical biometry and refinements in IOL power calculations have reduced random error and brought about improvements in the precision of refractive outcomes. Systematic error refers to results being systematically off-center on average and therefore compromising the accuracy of the outcomes. These results are amenable to correction in the same way that someone calibrates the crosshair of the sniper rifle and corrects the aim of the gun from the results of target B to the results of target C.

Optimizing the IOL constant corrects the systematic error of an IOL power formula in the same way as calibrating the crosshair of a gun. In the example above, the graph on the left side demonstrates a more diffuse spread around 0 and represents the spread of prediction error following a combination of applanation ultrasound with an appropriate IOL constant. When optical biometry is used, the spread of outcomes is tighter as the precision in axial measurement improves. Nevertheless, if the IOL constant is kept the same as for applanation ultrasound, the prediction error is systematically hyperopic (because applanation ultrasound systematically measures eyes shorter than optical biometry). The refractive outcomes in the graph with optical biometry and incorrect IOL constant are poor, worse than with applanation ultrasound (graph on left), with the average patient ending up with +0.5D hyperopia. When the appropriate IOL constant value is used, this resets the systematic error induced by the change in the biometry method, thus resetting the average prediction error to 0 [1] There is a multitude of sources of systematic error, arising from the biometry measurement to the IOL model used, so each combination of the biometry machine/IOL model yields a different IOL constant value.

P. Aristodemou (✉)
VRMCy Clinic, Limassol, Cyprus

The Cyprus Institute of Neurology and Genetics, Nicosia, Cyprus

J. Aramberri et al. (eds.), *Intraocular Lens Calculations*, Essentials in Ophthalmology,
https://doi.org/10.1007/978-3-031-50666-6_36

Table 36.1 Comparison of accuracy and precision in refractive outcomes

Target A Calibrated regular rifle	Target B Mis-calibrated Sniper rifle	Target C Calibrated Sniper rifle
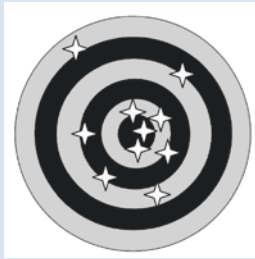		
Good ACCURACY Poor PRECISION	Poor ACCURACY Good PRECISION	Good ACCURACY Good PRECISION
		
Applanation ultrasound (US) Optimized IOL constant for US 55% within ±0.50D 85% within ±1.00D	Optimized biometry IOL constant for US 40% within ±0.50D 75% within ±1.00D	Optimized biometry (OB) Optimized IOL constant for OB 70% within ±0.50D 95% within ±1.00D

Factors That Affect the IOL Constant

Differences between IOL designs and biometry methods are all sources of systematic error and can displace the average prediction error away from 0.0D. These require an adjustment of the value (optimization) of the IOL constant in order to reset the mean prediction error to 0.0D. Therefore, each combination of the IOL model and biometry device may require a different IOL constant value.

A. The IOL Geometry

Even with in-the-bag IOL implantation, the post-operative IOL position and the location of the principal planes of the lens would depend on the geometry of the IOL. This may be related to the distribution of optical power between the anterior and the posterior IOL surfaces, the angulation of the haptics relative to the optic plane, and the shape, size, and material of the IOL(the material affects the refractive index and the softness of the material can affect the IOL thickness, eg hydrophilic acrylic is softer than hydrophobic acrylic and softer IOLs are often made thicker). Table 36.2 illustrates the location of the principal planes of a number of IOL optical designs.

The Alcon MA series (Alcon, Fort Worth, TX) is a good example of how the effective optical power varies after in-the-bag IOL implantation for the same optical power of an IOL and its impact on the IOL constant (Table 36.3).

Technical product information accessible at https://www.alcon.com/eye-care-products

B. Location of IOL implantation

Optimized constants for posterior chamber IOLs published by sites such as ULib (ocusoft.de/ulib/c1.htm) and IOL Con (iolcon.org) are specifically indicated for calculations when the IOL is implanted in the capsular bag (ULib has not been updated for some time at the time of writing this chapter). When the IOL is not implanted in the capsular bag, the optimized IOL constant may not be appropriate for that specific IOL position.

When an IOL is not implanted in the capsular bag, its anteroposterior position will affect its effective lens power. The more anterior the location of the IOL, the higher the effective power of the optic, and therefore, the nominal power of the IOL needs to be adjusted downwards in order to achieve the refractive target. This can be done in a

Table 36.2 Schematic location of principal planes with respect to the optical design of the IOL optic

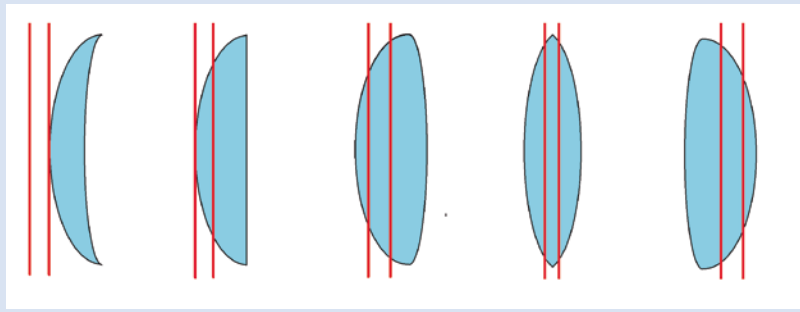

Convex Meniscus	Plano-Convex	Asymmetric anterior biconvex	Equiconvex *or* symmetric biconvex	Asymmetric posterior biconvex

Table 36.3 The influence of IOL design on effective lens power and IOL constant

IOL model	MA30 MA	MA60 AC	MA60 BM
Optic configuration	Asymmetric anterior biconvex	Asymmetric anterior biconvex	Asymmetric posterior biconvex
Haptic configuration	5° posterior angulation	10° posterior angulation	10° posterior angulation
Principal plane location	More anterior		More posterior
Effective lens power	Higher power		Lower power
ULIB optimized Hoffer Q pACD, Holladay 1 sf, SRK/T A-constant	5.46 1.64 118.7	5.67 1.90 119.2	6.08 2.33 119.8

number of ways. For anterior chamber IOLs, this is conventionally achieved by using their specific IOL constant, which is typically much lower than for posterior chamber IOLs. The same applies for iris-claw lenses, where the IOL constants for retro-pupillary fixation are higher than for fixation of the same IOL in front of the iris but lower than for other in-the-bag IOL models (iolcon.org).

When IOL constants for in-the-bag placement are used, sulcus implantation results in a myopic prediction error compared to intracapsular implantation. Various approaches have been described to address this systematic error:

(1) To reduce the IOL power by 0.5D or 1.0D for sulcus implantation in all cases: This would work in averaged-sized eyes and average powered IOLs but for high powered IOLs, the power reduction needs to be greater. The opposite applies to low-powered IOLs. By subtracting the same amount of power in all cases, this would undercorrect small eyes and overcorrect long eyes [2]. A slightly better rule of thumb is to reduce the implanted IOL power by 5% of that for in-the-bag implantation [3], but this approach is still suboptimal.

(2) To use IOL constants derived for sulcus implantation: The advantage of adjusting the IOL constant to match the new effective lens position is that the IOL power formula will predict the appropriate power adjustments with respect to the IOL power. This means that high-powered IOLs will have a greater reduction in IOL power, whereas low-powered IOLs will be affected less so. Surgeons should generate new IOL power constants for their IOL model of choice for sulcus implantation and have one calculation in their IOL calculation sheet so that the appropriate IOL power is available when sulcus implantation is indicated.

Obtaining the appropriate IOL constants for sulcus implantation can be done either by the conventional way or by collecting enough cases and performing optimization calculations [4] (see methodology), but this is often not possible as only very large centers would have the 100 or more eyes required with sulcus IOL implantation of the same IOL model. Alternatively, one can take into account the difference in average prediction error between in-the-bag implantation and sulcus

implantation for the same IOL model. This has been calculated at around −0.6 D of myopic shift for the sulcus for the same IOL power [3]. In the absence of enough cases with sulcus IOL implantation for formal IOL optimization, the optimized IOL constant for sulcus implantation can be derived by reducing the IOL constant for in-the-bag implantation by 0.47 (corresponding to the 0.6D myopic shift of sulcus implantation). The 0.47 reduction applies to the following IOL power formulae: Hoffer Q (pACD), Holladay 1 (sf), Barrett UII (surgeon factor), Holladay 2 (ACD), Haigis (a0), and the Olsen (ACD). For the IOL formulae using an "A constant" (SRK-T, T2, K6, and Kane formulae), the A constant should be reduced by 0.75 to obtain an optimized A constant for sulcus implantation (see Table 36.12). For example, the Alcon MA60AC 3-piece IOL has in-the-bag IOL constants of 5.67, 1.90, and 119.2 for the Hoffer Q, Holladay 1, and SRK/T, respectively (Table 36.3). For sulcus implantation, the estimated constants for the same IOL model are 5.20, 1.43, and 118.45 for the Hoffer Q, Holladay 1, and SRK/T, respectively.

Using a specific IOL constant for sulcus implantation has two main advantages: (1) the ease of use and (2) the automatic adjustment of the IOL power with respect to its effective lens position. When one uses a triple-optimized Haigis formula with real post-op data derived from sulcus IOL implantation, further refinements in precision can be obtained as the pre-operative ACD, Ks, and AL are used to predict the sulcus diameter, which, in turn, affects the compression of the IOL haptics in the sulcus and the posterior vault distance of the IOL optic [5].

(3) Perform back calculations for sulcus placement. Please refer to the chapter on out-of-the-bag IOL implantation by Dr. Jaime Aramberri.

There are other alternative fixation techniques, including (1) sulcus IOL haptic placement with the optic captured through the anterior capsulorrhexis opening, (2) sutured scleral fixation, and (3) sutureless scleral fixation at various distances behind the limbus.

Sulcus placement with optic capture through the anterior CCC has IOL constants that are closer in value to the ones needed for in-the-bag implantation [6]. On the other hand, intrascleral fixation of three piece IOLs appears to result in a more posterior IOL location to an in-the-bag reference, thus resulting in hyperopic prediction errors when IOL constants for in-the-bag implantation are used, so IOL constants for scleral fixation would need to be higher than those for in-the-bag implantation [7, 8].

C. Biometry

a. Axial Length

Axial length (AL) measurement in the days of ultrasound biometry was considered the primary source of prediction error [9]. Applanation ultrasound had additional issues with inducing errors because of the corneal flattening during measurement as this would measure the eye shorter [10]. Manufacturer's IOL constants were typically derived using applanation ultrasound as this was the most widely used approach. Immersion ultrasound offered superior outcomes as it left the eye undistorted during measurement but this was more labor intensive, and patients did not like the immersion water bath that was required for this ultrasound technique. When Zeiss developed the IOL Master, Prof Wolfgang Haigis, who was instrumental in its development, had calibrated the axial length measurements of the IOL Master against a high-definition 40 MHz immersion ultrasound machine. These made IOL Master AL measurements on average of the same magnitude as immersion ultrasound AL measurements (albeit with a smaller standard deviation, a narrower spread, offering improved precision) [11].

When subsequent biometry machines were developed by other manufacturers, their AL measurements were calibrated against the IOLMaster in order to meet FDA and other regulatory standards, so this makes the AL measurements between different biometers have very little to no systematic difference, translating to very similar outcomes. This applies both to low coherence

interferometry [12, 13] and swept-source OCT-based machines [14].

For some biometers, there are systematic differences in axial length measurement in longer eyes, and this stems from the fact that, currently, the axial length is measured as one singular measure despite it incorporates a number of media of optically different density (see Tables 36.4 and 36.5) for comparisons in axial length and ACD between biometers). When sum-of-segments axial length measurements become established in IOL power calculations, this would certainly translate to a change in IOL constant value but it may also make measurements between biometers more consistent [15] (see David Cooke's chapter on axial length measurements).

b. Keratometry

Any systematic differences in measuring corneal radii, even when they are seemingly very small, would have a disproportionate effect on shifting refractive outcomes away from an average 0.0D prediction error. This is because, in addition to measuring corneal power, keratometry measurements are used by IOL power formulae to predict the post-operative anterior chamber depth and effective lens position. Hence, systematic differences in keratometry have a double whammy effect on prediction error by both changing the corneal power and the predicted position of the IOL [44]. Therefore, any systematic difference should be factored into the IOL constant used for the specific biometry device (Table 36.6).

It must be stressed that Sim Ks from some topographers should not be used for IOL power calculations as these measurements can sometimes be very different from biometer Ks and result in a significant ametropic shift in refractive outcomes.

D. Less important factors: IOL Constant "Personalization"

Surgeons generally do not have significantly different "Personalised" IOL Constants from one another. The term "personalized IOL constant" dates back to a time when extracapsular cataract extraction (ECCE) was the standard surgical procedure [45]. For this surgical procedure, there are additional important variables and sources of error, compared to phacoemulsification with in-the-bag IOL implantation. In ECCE, surgeons typically performed a can opener capsulotomy, which was large and included radial capsular tears. Sometimes this permitted the placement of the lens in the bag and sometimes the lens was placed in the sulcus. Some surgeons were more reliable in achieving intracapsular implantation, whereas other surgeons routinely placed their IOLs in the sulcus regardless of the state of the anterior capsulotomy. The more anterior placement of the IOL causes the effective power of the IOL to increase and results in a more myopic deviation from an in-the-bag placement. This is why when using ECCE, it was important for every surgeon to determine their own "personalized" IOL constant, which would primarily depend on their routine IOL placement [46].

With phacoemulsification cataract extraction through a continuous curvilinear capsulorrhexis (CCC), IOL implantation has become more predictable, and therefore, any surgeon-derived variability has diminished [47, 48]. Provided that the CCC is smaller than the IOL optic (thus preventing any anterior optic prolapse) and that the posterior capsule remains intact at the end of the surgery, most surgeons appear to have very similar results. In a study of refractive outcomes looking at IOL constants, the IOL constants of 27 surgeons with more than 64 cases each and using the same biometer were very similar, and only one surgeon' constant deviated more than what is considered to be a clinically significant difference of IOL constant value from the average of all surgeons tested [1]. Another study used multilevel multivariate modeling to analyze 490,987 eyes of 351,864 patients, who had phacoemulsification cataract surgery by 2567 surgeons. It found that the surgeon accounted for only 4% of the variability in refractive outcomes, as opposed to 23% attributed to the patient level (patient-specific variables affecting both eyes and not attributed to the already measured biometry variables) and 73% to the eye level and other factors (e.g., biometry measurements, IOL power formula, etc) [49]. Therefore, the influence of the

Table 36.4 Comparisons in axial length measurements between different biometry machines (Refs [16–43])

Axial length	IOL Master5/500	Lenstar LS 900	AL Scan	Aladdin	Pentacam AXL	IOLMaster 700	Anterion	Argos Movu	Revo NX	Tomey OA 2000
IOL Master 5/500	X	NSDM NSDM NSDM +0.08 mm	NSDM	+0.04 mm NSDM	NSDM NSDM	NSDM NSDM Staphyloma: +0.095 mm NSDM		−0.026 mm		NSDM −0.06 −0.05
Lenstar LS 900		X	NSDM	NSDM NSDM	NSDM NSDM NSDM	Short AL: NSDM Med AL: NSDM Long AL: −0.05 mm −0.01 mm −0.01 mm	0.05 mm	−0.05 mm −0.05 mm	NSDM	0.03
AL scan			X							
Alladin				X		NSDM		−0.03		
Pentacam AXL					X	−0.07 mm		NSDM		
IOLM 700						X	NSDM −0.02 mm −0.07 mm	−0.03 mm −0.08 mm	NSDM	
HE Anterion							X			
Argos Movu								X		
Revo NX									x	
Tomey 2000										X

Numbers specify the mean difference of Top Row from Left Column, NSDM: No statistically significant difference between the means of AL

Table 36.5 Comparisons in ACD measurements between different biometry machines (Refs [16–43])

ACD	IOL Master5/500	Lenstar LS 900	AL Scan	Aladdin	Pentacam AXL	IOLMaster 700	Anterion	Argos Movu	Revo NX	Tomey OA 2000
IOL Master 5/500	X	NSDM NSDM +0.23 mm +0.13 mm	NSDM	NSDM	+0.05	−0.065 mm NSDM		−0.061 mm +0.20 mm		+0.05 mm −0.09 mm +0.01 mm
Lenstar LS 900		X	NSDM	NSDM	NSDM	−0.03 mm −0.07 mm NSDM	+0.05 mm	−0.03 mm		+0.05 mm
AL scan			X					+0.04 mm		
Alladin				X				+0.05 mm		
Pentacam AXL					X	−0.03 mm				
IOLM 700						X	+0.08 mm	NSDM +0.1 mm		
HE Anterion							X			
Argos Movu								X		
Revo NX									x	
Tomey OA2000										X

Numbers specify the mean difference of Top Row from Left Column, NSDM: No statistically significant difference between the means of ACD

Table 36.6 Comparisons in mean keratometry measurements between different biometry machines: (Refs [16–43])

Mean keratometry	IOL Master5/500	Lenstar LS 900	AL Scan	Aladdin	Pentacam AXL	IOLMaster 700	Anterion	Argos Movu	Tomey OA 2000
IOL Master 5/500	X	−0.16D −0.12D NSDM NSDM	+0.08D NSDM	+0.16D −0.09D NSDM NSDM	−0.1 D	−0.10D −0.078D NSDM		NSDM NSDM	NSDM −0.10D −0.13D
Lenstar LS 900		X	+0.11D	−0.04D NSDM	−0.19D −0.15D	NSDM −0.02D NSDM −0.11D	−0.26D	NSDM	+0.13D
AL Scan			X			−0.2D			
Alladin				X		NSDM		0.05D	
Pentacam AXL					X	+0.04D	NSDM	+0.280D	
IOLM 700						X	−0.06D NSDM NSDM −0.14D −0.37D	+0.075D +0.17D	
HE Anterion							X		
Movu								X	
Tomey OA 2000									X

Numbers specify the mean difference of Top Row from Left Column, NSDM: No statistically significant difference between the means of mean keratometry values

individual surgeon on the IOL constant is no longer such a critical factor as long as the other important factors have been taken into consideration, namely the biometry machine used and the IOL model implanted.

E. Spurious Factors Which Can Result in Incorrect IOL Constant Values

a. The Short Vision Lane Issue

An often overlooked source of bias is the postoperative refraction. Our IOL selection is based on a target refraction for an optical correction that achieves emmetropia, i.e., a far point at infinity. Nevertheless, our vision lanes have finite dimensions. Although the standard is set at 6 m, some vision lanes can be 4 m in length or shorter. This is another source of bias, which can affect the refractive outcomes as the refractionist tests at a far point less than 6 m. It is very important to stress that short lanes would give erroneous hyperopic outcomes, and these must NOT be used to optimize IOL constants; otherwise, these incorrect IOL constants would result in patients ending up myopic on average.

If the post-op refraction data are derived from testing at a short vision lane, the refraction can easily be adjusted to a far point at 6 m by subtracting the difference in vergence between the two far points, using the formula or Table 36.7 [50].

$$\left(\text{Spherical equivalent at 6 metres}\right) = \left(\text{Spherical equivalent at } \boldsymbol{X} \text{ metres}\right) + \frac{1}{6} - \frac{1}{\boldsymbol{X}}$$

b. The "Home Court Advantage" Issue

Data from subjective refraction may misleadingly show improved outcomes of the IOL formula used by the surgeon. This is because of the inherent bias of subjective refraction, as the subjectiveness of this test is also derived from the part of the refractionist. Therefore, patients with

Table 36.7 Adjustment of post-op refraction spherical equivalent derived from short lane testing

Lane length	6 m	5 m	4 m	3.5 m	3 m
Correction to 6 m	N/A	= 0.17 − 0.20 = −0.03D Subtract 0.03D	= 0.17 − 0.25 = −0.08 Subtract 0.08D	= 0.17 − 0.29 = 0.12 Subtract 0.12D	= 0.17 − 0.33 = −0.15 Subtract 0.15D

low refractive errors and small pupils who may be able to see 20/20 may be labeled as having a 0.00 D refractive error. This gives a false advantage to the IOL power formula used by the surgeon, as the surgeon often chooses the IOL power giving a target refraction closest to 0, and the refractionist may label the patient as having 0 refractions, thus erroneously matching a 0 target with a 0 refraction. Over repeated cases, the IOL formula in question would have more target refractions closer to 0 compared to other formulae that were not used thus giving the formula a "home court advantage" a term coined by Dr. David Cooke of Great Lakes Eye Care, St. Joseph, Michigan. This may explain why when comparing IOL formulae calculations, the best-performing formula is often the one actually used by the surgeon for the power calculation.

Although subjective refraction is still considered by many the gold standard, this a topic often discussed among the members of the IOL power club, and some members feel that a calibrated autorefractor may be a better approach for outcome studies as it would be less prone to the subjective sources of bias discussed above. In an ideal scenario, both subjective refraction and autorefraction would be performed with the former used for any spectacle prescriptions and the later for audit purposes and IOL constant refinement.

The Methodology for Deriving IOL Constants

Data and Sample Size Requirements

The sample of eyes used for IOL constant optimisation should have undergone uncomplicated phacoemulsification with an in-the bag IOL. The capsulorrhexis size should be smaller than the optic, with no post-operative prolapse of the IOL optic through the bag, no corneal sutures, and a post-op visual acuity of logMAR 0.2 or better (≥7/10, ≥6/9, ≥20/30 decimal) in order to achieve accurate subjective refractions. There should be no attempt to select eyes with respect to their biometric variables (i.e., the sample should contain a non-selected and non-biased distribution of axial lengths, keratometry, ACD, etc). Care must be taken not to use cases where the IOL has been implanted back-to-front. There should be no history of refractive corneal or any other ophthalmic surgery. Significant corneal pathology, such as keratoconus, pterygium, or corneal scarring, should be excluded. All post-operative subjective refractions should ideally be refined using a red/green duochrome test. Please note the issues raised regarding the length of the vision lane, if this is shorter than 6 m, an appropriate correction should be applied for that working distance. The essential/*ideal* set of data would include (1) Axial Length, (2) K1 and K2, (3) *CCT,* (4) ACD*,* (5) LT*,* (6) *Horizontal Corneal Diameter* (HCD)*,* (7) *Gender,* (8) IOL Model, (9) IOL Power, (10) Refraction, and (11) Vision lane distance. Some IOL power formulae require post-op biometric measurements for optimization so (12) biometrically measured post-op ACD is essential for optimizing the Olsen, Castrop, and K6. Formulae using a thick lens model can require the physical characteristics of the IOL model and for some formulae, even the variation of these across the IOL power range. It is also important to note that the same biometry machine model must be used for all cases and that the IOL derived would be specific for use with that biometry machine model.

The general consensus is that 100 eyes are enough to optimize IOL constants. It is said that 250 eyes are needed for triple optimization of the Haigis formula. Figures 36.1, 36.2, 36.3, and 36.4 show the fluctuation of IOL constants (for the Hoffer Q, Holladay 1, SRK/T, Haigis) with

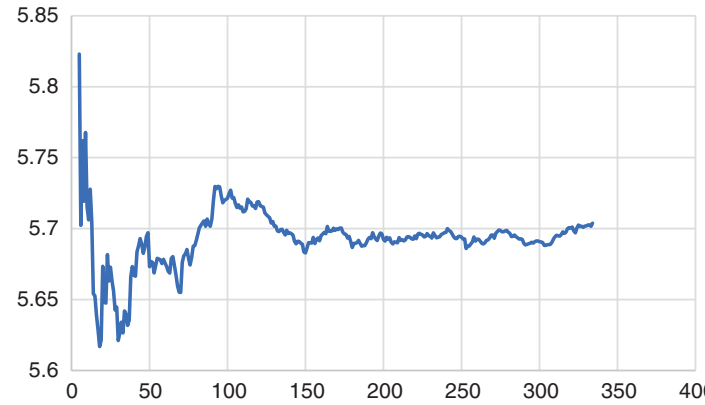

Fig. 36.1 ACD (Hoffer Q) and increasing sample size

Fig. 36.2 sf (Holladay 1) and increasing sample size

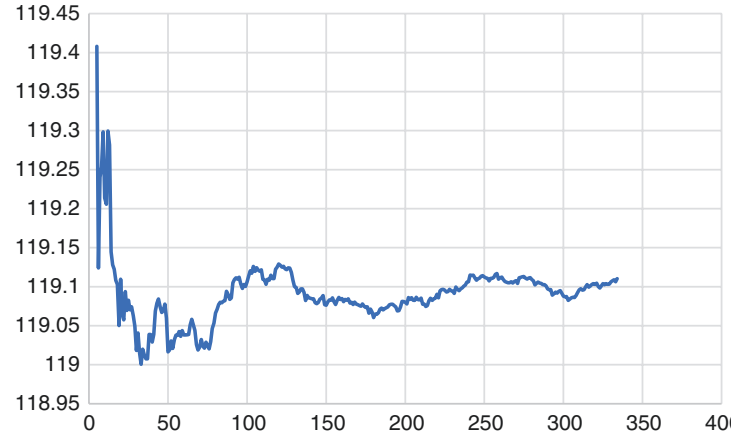

Fig. 36.3 A constant (SRK/T) and increasing sample size

respect to an increasing sample of eyes, starting from 10 eyes up to 330 eyes. The data are from my private practice using the same IOL model, and for this process, they are analyzed in a randomized order without removing outliers from the optimization process as in reality; it is difficult to detect outliers from the outset before having a large enough sample.

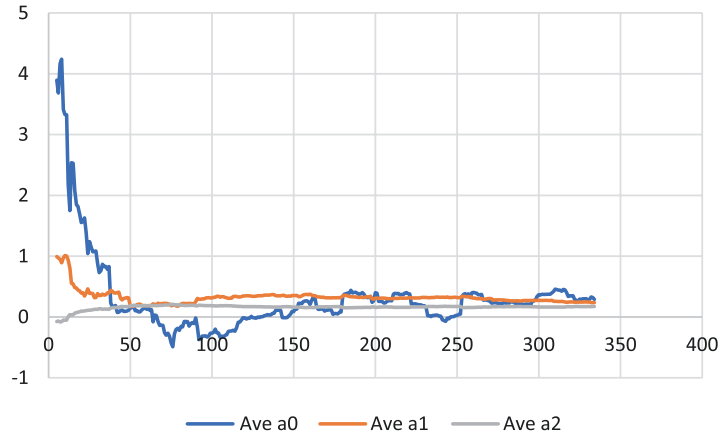

Fig. 36.4 Haigis constants (a0, a1, and a2) and increasing sample size

Previous studies on theoretical refractive outcomes suggest that for the Hoffer Q and Holladay 1, IOL constant change within ±0.05 and for the SRK/T change within ±0.10 has no significant impact on refractive outcomes [1]. Based on the above, 100 eyes should be enough to calculate IOL constants. Figure 36.4 shows the triple optimization for the Haigis may need fewer than 250 eyes. The a1 and a2 constants representing the regression coefficients (slope) for ACD and AL, respectively, are the first to stabilize, followed by the intersect (a0).

Optimization of Single-Variable IOL Power Formulae

Most IOL power formulae contain only one IOL constant. For the vast majority of single-variable formulae, the IOL constant is optimized by finding the IOL constant value for each eye in order to achieve a match between predicted refraction and post-op refraction for the IOL power used for that eye. This is repeated for all the eyes in the sample used, and the values are averaged to give the optimized IOL constant.

A. Standard Iterative Approach for Optimizing Single-Variable IOL Power Formulae

The code has been published for some IOL formulae [11, 51–53], and this can be used to perform these calculations (Please note that the original papers for the Hoffer Q, the Holladay 1, and SRK/T had typographical errors in the code, which were later corrected by published letters and errata) [54, 55]. After transcribing the code on a spreadsheet, one can use pre-op biometry measurements to calculate the IOL power for a specific refractive outcome. If surgeons choose to use this approach, they should exercise particular care to avoid any transcription errors in the formula code, which would result in incorrect calculations. Textbox 36.1 provides a calculation guide for optimizing the third generation IOL power formulae.

Box 36.1 Calculation Guide for Optimizing Hoffer Q, Holladay 1, SRK/T and Haigis Formulae

The tables below contain the code for each of the formulae Hoffer Q, Holladay 1, SRK/T and Haigis (Tables 36.8, 36.9, and 36.10). Each table represents a separate sheet in an Excel workbook (Microsoft Corporation, version 2010 or newer). Table 36.8 is to be used for third generation IOL constant optimization sheet. This sheet should be named "**Constant optimization**". Table 36.9 is for the double regression calculation for the Haigis formula optimization sheet. This sheet should be named "**Haigis optimization**". Table 36.10 is for the IOL power calculation sheet,

Table 36.8 SHEET 1: IOL Constant Optimisation Sheet [11, 44, 51–55]

Column	Row 1	Row 2
A	Case No	*Input Data* (case 1,2,3,4, etc)
B	Axial Length	*Input Data* (in mm)
C	K1	*Input Data* (in D)
D	K2	*Input Data* (in D)
E	Pre op ACD	*Input Data* (in mm)
F	Implanted IOL power	*Input Data* (in D)
G	Desired Post op SEq	*Input Data* (in D)
H	Post op Sphere	*Input Data* (in D)
I	Post Op Cylinder	*Input Data* (in D)
J	Post op Axis	*Input Data* (in degrees)
K	Post op Spherical Equivalent	=H2+(I2/2)
L	Mean K	=(C2+D2)/2
Hoffer Q Optimisation		
M	Calculated "ACD" Constant For each eye	Use the GoalSeek function in a Macro to calculate the ACD value so that the Calculated IOL power (**V**) matches the Implanted IOL power (**F**) and use the Post op RX result values (**K**) to populate the Desired Rx SE (**Q**). This will find the ACD constant for each case so that the calculated IOL power matches the IOL power used.
N	Axial length	**=B2**
O	Mean K	**=L2**
P	Vertex distance	*=12 (twelve mm is the standard vertex distance)*
Q	Post op op SE used as desired Rx	**=K2**
R	*M*	=IF(**B2**<23,1,-1)
S	*G*	=IF(**B2**<23,28,23.5)
T	Predicted ACD	=**M2**+0.3*(**N2**-23.5)+(TAN(**O2***PI()/180))^2+(0.1 ***R2***(23.5-**N2**)^2*(TAN(0.1*(**S2**-**N2**)^2*PI()/180)))-0.99166
U	Expected Rx SEq for the IOL selected	=(1.336/(1.336/(1336/(**N2**-**T2**-0.05)-**F2**)+(**T2**+0.05)/1000))-O2
V	Calculated IOL power	=(1336/(**N2**-T2-0.05))-(1.336/((1.336/(**O2**+**Q2**/(1-0.001*P2***Q2**)))-((**T2**+0.05)/1000)))
Holladay 1 Optimisation		
W	Calculated "SF" constant for each eye	Use the GoalSeek function in a Macro to calculate the SF value so that the Calculated IOL power (**AF2**) matches the Selected IOL power (**F2**) and use the Post op RX result values (**K2**) to populate the Desired Rx SE (**AC2**). This will find the SF constant for each case so that the calculated IOL power matches the IOL power used.
X	Axial length	**=B2**
Y	ALm	=**X2**+0.2
Z	Mean K	**=L2**
AA	R-H1	=337.5/**Z2**
AB	Vertex distance	*=12 (twelve mm is the standard vertex distance)*
AC	Post op op SE used as desired Rx	**=K2**
AD	Ag	=12.5***X2**/23.45
AE	ACD post K	=0.56+**AA2**-SQRT(**AA2**^2-**AD2**^2/4)

Table 36.8 (continued)

Column	Row 1	Row 2
AF	Calculated IOL power	=1336*(1.336***AA2**-1/3*Y2-0.001***AC2***(**AB2***(1.336***AA2**-1/3***Y2**)+**Y2***AA2**))/((**Y2**-**AE2**-**W2**)*(1.336***AA2**-1/3*(**AE2**+**W2**)-0.001***AC2***(**AB2***(1.336***AA2**-1/3*(**AE2**+**W2**))+(**AE2**+**W2**)*AA2**)))
AG	Expected Rx for the IOL selected	=(1336*(1.336***AA2**-(4/3-1)***Y2**)-**F2***(**Y2**-**AE2**-**W2**)*(1.336***AA2**-(4/3-1)*(**AE2**+**W2**)))/(1.336*(12*(1.336***AA2**-(4/3-1)***Y2**)+**Y2***AA2**)-0.001***F2***(**Y2**-**AE2**-**W2**)*(12*(1.336***AA2**-(4/3-1)*(**AE2**+**W2**))+(**W2**+**AE2**)*AA2**))
AH	Predicted ACD	=**W2**+**AE2**
SRK-T Optimisation		
AI	Axial Length	=**B2**
AJ	Calculated A-constant	Use the GoalSeek function in a macro to calculate the A constant value so that the calculated expected refraction (**AX2**) matches the post op refraction (**K2**). This will find the A-constant for each case so that the calculated expected refraction matches the post op refraction for the IOL power used.
AK	ACD constant	=0.62467***AJ2**-68.747
AL	Mean K	=**L2**
AM	Radius – SRK/T	=337.5/**AL2**
AN	LCOR	=IF(**AI2**>24.2,-3.446+1.716***AI2**-0.0237***AI2**^2,**AI2**)
AO	Cw	=-5.41+0.58412***AN2**+0.098***AL2**
AP	H	=**AM2**-SQRT(**AM2**^2-**AO2**^2/4)
AQ	ACD estimate	=**AP2**+**AK2**-3.336
AR	Vertex distance	*=12 (twelve mm is the standard vertex distance)*
AS	na	=1.336
AT	nc	=1.333
AU	ncm1	=0.333
AV	Retinal thickness	=0.65696-0.02029***AI2**
AW	LOPT	=**AI2**+**AV2**
AX	Expected RX for IOL selected	=(1336*(**AS2***AM2-AU2***AW2**)-**F2***(**AW2**-**AQ2**)*(**AS2***AM2-AU2***AQ2**))/(**AS2***(12*(**AS2***AM2-AU2***AW2**)+**AW2***AM2**)-0.001***F2***(**AW2**-**AQ2**)*(12*(**AS2***AM2-AU2***AQ2**)+**AQ2***AM2**))
AY	IOL for emmetropia	=(1000***AS2***(**AS2***AM2-AU2***AW2**))/((**AW2**-**AQ2**)*(**AS2***AM2-AU2***AQ2**))
Haigis Optimisation		
AZ	a0	Leave blank to populate later with the optimized a0 value – in order to ensure that the mean prediction error is 0
BA	a1	Leave blank to populate later with the optimized a1 value – In order to ensure that the mean prediction error is 0
BB	a2	Leave blank to populate later with the optimized a2 value – In order to ensure that the mean prediction error is 0
BC	Pre op ACD	=**E2**
BD	Axial length	=**B2**
BE	RC1	=((1.3375-1)/**L2**)*1000
BF	Desired Rx matched to post op Rx	=**BO2**
BG	d	Use the GoalSeek function in a macro to calculate the "d" value so that the calculated IOL power (**BM2**) matches the selected IOL power (**BP2**) *(this is the column of data used in conjunction with pre op ACD (BC) and axial length (BD) to perform double linear regression in order to calculate a0, a1 and a2)*
BH	PC	=(1331.5-1000)/**BE2**
BI	Vertex distance	*=12 (twelve mm is the standard vertex distance)*

(continued)

Table 36.8 (continued)

Column	Row 1	Row 2
BJ	Rx for VD	=BF3/(1-**BI3***0.001***BF3**)
BK	T1	=1336*(1336-**BR2***(**BD2**-**BG2**))
BL	T2	=1336*(**BD2**-**BG2**)+**BG2***(1336-**BR2***(**BD2**-**BG2**))
BM	Calculated IOL power	**=BK2**-**BL2**
BN	Z1	=1336*(1336-**BR2***(**BD2**-**BG2**))
BO	Z2	=1336*(**BD2**-**BG2**)+**BG2***(1336-**BR2***(**BD2**-**BG2**))
BP	Z	**=BN2/BO2**
BQ	Post op refraction	**=K2**
BR	Implanted IOL	**=F2**
DATA CHECK FOR SUCCESSFUL ITERATION AND OPTIMISED IOL CONSTANTS		
BS	PE Hoffer	**=K2-U2 This value should be 0 in every case, if the iteration calculation was successful**
BT	PE Holladay 1	**=K2-AG2 This value should be 0 in every case, if the iteration calculation was successful**
BU	PE SRK/T	**=K2-AX2 This value should be 0 in every case, if the iteration calculation was successful**
BV	BLANK	
BW	Use for labels	Cell BW2: "Optimized pACD" Cell BW3: "Optimized SF" Cell BW4: "Optimized A Constant"
BX	IOL constant values	Cell BX2: =AVERAGE(**M:M**) Cell BX3: =AVERAGE(**W:W**) Cell BX4: =AVERAGE(**AJ**:**AJ**)

Table 36.9 SHEET 2: Double linear regression for Haigis Optimisation IOL Constant Optimisation Sheet [11, 44]

A	ACD (X_1)	copy – paste (values) column BC from sheet 1
B	Axial Length (X_2)	copy – paste (values) column BD from sheet 1
C	"d" (Y)	copy – paste (values) column BG from sheet 1
D	(X_1-avX_1) * (Y-avY)	=(A2-(AVERAGE(A:A)))*(C2-(AVERAGE(C:C))) make sure you use all the brackets as specified
F	(X_2-avX_2) * (Y-avY)	=(B2-(AVERAGE(B:B)))*(C2-(AVERAGE(C:C))) make sure you use all the brackets as specified
G	(X_1-avX_1) * (X_2-avX_2)	=(A2-(AVERAGE(A:A)))*(B2-(AVERAGE(B:B))) make sure you use all the brackets as specified
H	(X_1-avX_1)^2	=POWER((A2-(AVERAGE(A:A))),2) make sure you use all the brackets as specified
I	(X_2-avX_2)^2	=POWER((B2-(AVERAGE(B:B))),2) make sure you use all the brackets as specified
J,K	BLANK	
L	Use for labels for M values	L5: "$\sum$ (X_1-avX_1)^2 " L6: "$\sum$ (X_2-avX_2)^2" L7: etc….
M5	Cell M5 " $\sum$ (X_1-avX_1)^2 "	=sum(H:H)
M6	Cell M6 "$\sum$ (X_2-avX_2)^2 "	=sum(I:I)
M7	Cell M7 "$\sum$((X_1-avX_1) * (Y-avY))"	=sum(D:D)
M8	Cell M8 "$\sum$((X_2-avX_2) * (Y-avY))"	=sum(F:F)
M9	Cell M9 "$\sum$((X_1-avX_1) * (X_2-avX_2))"	=sum(G:G)
M10	Cell M10 "Haigis Constants"	Blank
M11	Cell M11 "a0"	=(AVERAGE(C:C))-((AVERAGE(A:A))*M12)-((Average(B:B))*M13) "the intersect on the Y axis"
M12	Cell M12 "a1"	=((M6*M7)-(M9*M8))/((M5*M6)-(M9*M9)) "the ACD coefficient"
M13	Cell M13 "a2"	=((M5*M8)-(M9*M7))/((M5*M6)-(M9*M9)) "the AL coefficient"

Table 36.10 SHEET 3: IOL Power calculations using Optimised IOL constants [11, 44, 51–55]

Column	Row 1	Row 2
Enter data		
A	Case No	*Input Data* (case 1,2,3,4, etc)
B	Axial Length	*Input Data* (in mm)
C	K1	*Input Data* (in D)
D	K2	*Input Data* (in D)
E	Pre op ACD	*Input Data* (in mm)
F	Implanted IOL power	*Input Data* (in D)
G	Desired Post op SEq	*Input Data* (in D)
H	Post op Sphere	*Input Data* (in D)
I	Post Op Cylinder	*Input Data* (in D)
J	Post op Axis	
K	Post op Spherical Equivalent	=H2+(I2/2)
L	Mean K	=(C2+D2)/2
Hoffer Q calculations with an optimised IOL constant		
M	Optimised "ACD" Constant	For every case, use the optimized ACD constant value from **Sheet 1, Cell BX2**
N	Axial Length	**=B2**
O	Mean K	**=L2**
P	Vertex Distance	*=12 (twelve mm is the standard vertex distance)*
Q	Desired Rx	**=G2**
R	*M*	=IF(**B2**<23,1,-1)
S	*G*	=IF(**B2**<23,28,23.5)
T	Predicted ACD	=**M2**+0.3*(**N2**-23.5)+(TAN(**O2***PI()/180))^2+(0.1 *__R2__*(23.5-**N2**)^2*(TAN(0.1*(**S2**-**N2**)^2*PI()/180)))-0.99166
U	Expected Rx SEq for the IOL selected	=(1.336/(1.336/(1336/(**N2**-**T2**-0.05)-**F2**)+(**T2**+0.05)/1000))-O2
V	Calculated IOL Power for Desired Rx	=(1336/(**N2**-T2-0.05))-(1.336/((1.336/(**O2**+**Q2**/ (1-0.001*__P2__*__Q2__)))-((**T2**+0.05)/1000)))
Holladay 1 calculations with an optimised IOL constant		
W	Optimised SF constant	For every case, use the optimized SF constant value from **Sheet 1, Cell BX3**
X	Axial Length	**=B2**
Y	ALm	=**X2**+0.2
Z	Mean K	**=L2**
AA	R-H1	=337.5/**Z2**
AB	Vertex Distance	*=12 (twelve mm is the standard vertex distance)*
AC	Desired Rx	**=G2**
AD	ag	=12.5*__X2__/23.45
AE	ACD post K	=0.56+**AA2**-SQRT(**AA2**^2-**AD2**^2/4)
AF	Calculated IOL Power for Desired Rx	=1336*(1.336*__AA2__-1/3*Y2-0.001*__AC2__*(__AB2__*(1.336*__AA2__-1/3*__Y2__)+__Y2__*__AA2__))/ ((__Y2__-__AE2__-__W2__)*(1.336*__AA2__-1/3*(__AE2__+__W2__)-0.001*__AC2__*(__AB2__*(1.336*__AA2__-1/3*(__AE2__+__W2__))+(__AE2__+__W2__)*__AA2__)))
AG	Expected Rx for the IOL selected	=(1336*(1.336*__AA2__-(4/3-1)*__Y2__)-__F2__*(__Y2__-__AE2__-__W2__)*(1.336*__AA2__-(4/3-1)*(__AE2__+__W2__)))/(1.336*(12*(1.336*__AA2__-(4/3-1)*__Y2__)+__Y2__*__AA2__)-0.001*__F2__*(__Y2__-__AE2__-__W2__)*(12*(1.336*__AA2__-(4/3-1)*(__AE2__+__W2__))+(__W2__+__AE2__)*__AA2__))
AH	Predicted ACD	**=W2+AE2**

(continued)

Table 36.10 (continued)

Column	Row 1	Row 2
SRK/T calculations with an optimised IOL constant		
AI	Axial Length	**=B2**
AJ	Optimized A-Constant	For every case, use the optimized A-Constant value from **Sheet 1, Cell BX4**
AK	ACD Constant	=0.62467*__AJ2__-68.747
AL	Mean K	**=L2**
AM	Radius – SRK/T	=337.5/__AL2__
AN	LCOR	=IF(__AI2__>24.2,-3.446+1.716*__AI2__-0.0237*__AI2__^2,__AI2__)
AO	Cw	=-5.41+0.58412*__AN2__+0.098*__AL2__
AP	H	=__AM2__-SQRT(__AM2__^2-__AO2__^2/4)
AQ	ACD estimate	=__AP2__+__AK2__-3.336
AR	Vertex Distance	*=12 (twelve mm is the standard vertex distance)*
AS	na	=1.336
AT	nc	=1.333
AU	ncm1	=0.333
AV	Retinal Thickness	=0.65696-0.02029*__AI2__
AW	LOPT	=__AI2__+__AV2__
AX	Expected RX for IOL selected	=(1336*(__AS2__*__AM2__-__AU2__*__AW2__)-__F2__*(__AW2__-__AQ2__)*(__AS2__*__AM2__-__AU2__*__AQ2__))/(__AS2__*(12*(__AS2__*__AM2__-__AU2__*__AW2__)+__AW2__*__AM2__)-0.001*__F2__*(__AW2__-__AQ2__)*(12*(__AS2__*__AM2__-__AU2__*__AQ2__)+__AQ2__*__AM2__))
AY	IOL for Emmetropia	=(1000*__AS2__*(__AS2__*__AM2__-__AU2__*__AW2__))/((__AW2__-__AQ2__)*(__AS2__*__AM2__-__AU2__*__AQ2__))
Haigis calculations with an optimised IOL constants		
AZ	a0	For every case, use the optimized a0 value from Sheet 2, Cell M11
BA	a1	For every case, use the optimized a1 value from Sheet 2, Cell M12
BB	a2	For every case, use the optimized a2 value from Sheet 2, Cell M13
BC	Pre op ACD	**=E2**
BD	Axial Length	**=B2**
BE	RC1	=((1.3375-1)/__L2__)*1000
BF	Desired Rx	**=G2**
BG	d	**=AZ2+BA2*BC2+BB2*BD2**
BH	PC	=(1331.5-1000)/__BE2__
BI	Vertex Distance	*=12 (twelve mm is the standard vertex distance)*
BJ	Rx for VD	=BF3/(1-__BI3__*0.001*__BF3__)
BK	T1	=1336*(1336-__BR2__*(__BD2__-__BG2__))
BL	T2	=1336*(__BD2__-__BG2__)+__BG2__*(1336-__BR2__*(__BD2__-__BG2__))
BM	Calculated IOL power	**=BK2-BL2**
BN	Z1	=1336*(1336-__BR2__*(__BD2__-__BG2__))
BO	Z2	=1336*(__BD2__-__BG2__)+__BG2__*(1336-__BR2__*(__BD2__-__BG2__))
BP	Z	**=BN2/BO2**
BQ	Post op Refraction	**=K2**
BR	Implanted IOL	**=F2**
BS	Expected Rx with Implanted IOL	=(__BP2__-__BH2__)/(1+(__BP2__-__BH2__)*(12*0.001))
REFRACTIVE OUTCOME ANALYSIS USING OPTIMISED IOL CONSTANTS		
BT	PE Hoffer	**=K2-U2**
BU	PE Holladay 1	**=K2-AG2**
BV	PE SRK/T	**=K2-AX2**
BW	PE Haigis	**=K2-BS2**
BX	Absolute PE Hoffer	=ABS(__K2-U2__)

Table 36.10 (continued)

Column	Row 1	Row 2
BY	Absolute PE Holladay 1	=ABS(**K2-AG2)**
BZ	Absolute PE SRK/T	=ABS(**K2-AX2)**
CA	Absolute PE Haigis	=ABS(**K2-BS2)**
CB	Blank	
CC	Labels for CA	CC2: "Hoffer Q" CC3: "Holladay 1" CC4: "SRK/T" CC5: "Haigis"
CD	MNE Values	CD2: =Average(BT:BT) CD3: =Average(BU:BU) CD4: =Average(BV:BV) CD5: =Average(BW:BW)
CE	MAE Values	CE2: =Average(BX:BX) CE3: =Average(BY:BY) CE4: =Average(BZ:BZ) CE5: =Average(CA:CA)

Note: The average MNE values should be very close to 0 if the optimized IOL constants are correct and appropriate for this sample

using the derived IOL constants. This sheet should be named "**Calculation with opt. constants**".

For each formula, there is an optimization and a calculation section. The code is formatted to be used on an excel spreadsheet. It must be stressed that this is a research tool and it must not be used on actual calculations on patients. Also, before using the formulae to optimise constants, one should check for any transcription errors and following that, validate the outcomes against an approved IOL calculator containing the above IOL power formulae.

Each column of the table should be transposed into a row. Entries in the first column of the table are the column letters, starting with A. Entries in the second column of the table are the headers. Entries in the third column represent the formula code. Once the newly transposed first row containing the letters A, B, C is confirmed to identify with the column letters, this first row can be deleted, leaving the headers row as the first row and the code row as the second row. The code can be transferred to the rest of the rows automatically using excel. Data should then be entered for columns A to J. The other columns will automatically calculate various parts of each IOL formula on sheet 1 (Table 36.8).

The columns representing IOL constants are empty. One then uses the Goal Seek function on Microsoft Excel to calculate the IOL constant by iteration for each case so that the calculated IOL power matches the IOL power used to achieve the actual post-operative refraction. This is the IOL constant value for each case that would have resulted in the IOL power that was actually used to reach the observed refractive prediction. Please see the macro code on Table 36.11, which automates the process for any number of eyes. The macro can be activated by a button which can be designed with excel. It is worth noting that the optimization macro is coded to use a sample of 250 cases (rows 2 to 251). If you use a different number, change the last number in the code. Excel allows the insertion of buttons in each sheet, which can be linked to each macro.

First, the "clear calculations" macro should be used. Then, by running the optimization macro, the IOL constant will be calculated for each case to achieve 0 prediction error for the IOL power used. When this is done on 100 or so cases, all the IOL constants can be averaged and this represents the optimised IOL constant, which can be used in Sheet 3 for every new case, as long as the same IOL model and biometer is used.

Table 36.11 Macro codes for IOL constant optimization

Name of macro	Code
Sheet 1: "Clear Calculations" Macro	Sub ClearCalculations() Sheets("Constant optimization").Select Range("BH2:BH336").Select Selection.ClearContents Range("AK2:AK336").Select Selection.ClearContents Range("X2:X336").Select Selection.ClearContents Range("N2:N336").Select Selection.ClearContents Sheets("Input Data for Optimisation").Select End Sub
Sheet 1: "Optimization" Macro	Sub Optimization() Sheets("Constant optimization").Select Dim k For k = 2 To 251 Cells(k, "BM").GoalSeek Goal:=Cells(k, "BR"), ChangingCell:=Cells(k, "BG") Next k Dim q For q = 2 To 251 Cells(q, "V").GoalSeek Goal:=Cells(q, "F"), ChangingCell:=Cells(q, "M") Next q Dim s For s = 2 To 251 Cells(s, "AF").GoalSeek Goal:=Cells(s, "F"), ChangingCell:=Cells(s, "W") Next s Dim a For a = 2 To 251 Cells(a, "AX").GoalSeek Goal:=Cells(a, "K"), ChangingCell:=Cells(a, "AJ") Next a End Sub

Haigis Formula

The code on Table 36.9 contains the mathematical calculations which perform double regression and derive the a0 a1 and a2. For the sheet named "**Haigis optimization**", one copy pastes the values of measured pre op ACD (column E on Sheet 1), measured Axial Length (column B on sheet 1) and optimised "d" (column BG on Sheet 1). The former two are X1 and X2 respectively and "d" is Y. Sheet 2 will automatically perform double regression calculations to derive a0 (intersect), a1 (ACD coefficient) and a2 (AL coefficient). These can then populate the a0 a1 and a2 columns AZ, BA, BB on Sheet 3 "**Calculation with opt.constants**".

B. A Maths-Free Approach for Obtaining and Refining IOL Constants

When starting to use a new IOL model, it is important to find the optimized IOL constants for the biometry machine used. These can be obtained from the biometry machine representative, the IOL manufacturer, or a public database, such as the IOL Con website (iolcon.org). All surgeons carrying out cataract surgery should audit their refractive outcomes, and they should confirm that their mean prediction error is very close to 0. If this is not close to 0, one can use the mathematical approaches described above. Alternatively, for small refinements of an IOL constant, there is a very simple approach, which can be equally effective.

For the formulae Hoffer Q, Holladay 1, Barrett Universal, Holladay 2, the Olsen, and the Haigis

(a0), a change of 1 unit of IOL constant translates to 1.3D of prediction change at the spectacle plane [56]. Vice versa, for every 1.0D change in mean prediction error, the IOL constant changes by 0.77 in magnitude for the Hoffer Q pACD, the Holladay 1 sf, the Barrett Surgeon Factor, the Holladay 2 ACD, the Olsen ACD, and the Haigis a0. For the "A constants" for each 1D of change in MPE, the SRKT A constant, the T2 A constant, and the Kane A constant will change by 1.25 units. Table 36.12 below summarises these changes and provides examples. The Haigis should ideally be triple optimized (i.e., modifying a0, a1, and a2 using a double regression approach as discussed later). With this method, only a0 is modified, so this approach is not recommended for optimizing the Haigis formula. Please refer to the section on triple optimization of the Haigis.

C. Optimizing Single-Variable Unpublished IOL Power Formulae

For many of the newer IOL power formulae, the code is not available in order to perform the mathematical approach described above. There is another approach to do that. By having access to an IOL calculator which contains the hidden formula code, one can set up a bot/macro/script to perform repeat IOL power calculations for the IOL power used and vary the IOL constant iteratively for each eye, in order to match its predicted refraction to the post of refraction. By then averaging these values for a sample of eyes, one obtains the optimized IOL constant.

Some members of the IOL power club have offered to help surgeons with optimizing their IOL constants. Dave Cooke can be contacted at dcooke@greateyecare.com. He asks for at least 100 eyes meeting the inclusion/exclusion criteria above. He can send a spreadsheet that can be filled in.

IOL Formulae Requiring a Different Approach to Optimizing Their Constant(s)

A. The Haigis Formula

The Haigis formula uses three IOL constants *a*0, *a*1, and *a*2. It is very important that all three constants are optimized for the IOL used [11]. Compared to the third generation IOL power formulae, the Haigis formula uses a more accurate method for predicting the effective lens position (ELP) by the use of a regression formula that takes into account the pre-op ACD and axial length when predicting the ELP. *a*0, *a*1, and *a*2 are the intersect and the coefficients for the ACD and AL, respectively.

$$\mathbf{ELP} = \boldsymbol{a0} + \boldsymbol{a1} * \boldsymbol{ACD} + \boldsymbol{a2} * \mathbf{AL}$$

For the optimization, 250 eyes are used and the ELP is back-calculated for each eye to match the IOL power used for the post-op refraction. Then, by performing double linear regression using these theoretical ELPs against ACD and AC, the values for a0 as the intersect, the a1 as the ACD coefficient, and the *a*2 as the AL coefficient (see Textbox 1 for details on the methodology). Optimising the *a*1 and the *a*2, this corrects any systemic bias in estimating the ELP for the specific IOL, across the pre-op ACD and pre-op AL ranges.

In addition, it is important to note that for all thin-lens IOL power formulae, the calculated effective lens position is the theoretical position of an infinitesimally thin lens, which would yield the same effective power as the implanted IOL. The effective lens position is NOT the actual post-operative anterior chamber depth.

B. The Olsen Formula

The Olsen formula is a thick lens formula and has separated the constants into two categories [57]. The first category has to do with the actual dimensions and physical properties of the IOL, which are typically provided by the IOL manufacturer: the refractive index, the anterior and posterior radius of curvature of the optic, the central IOL thickness, and the spherical aberration of the IOL (SA) (the IOL thickness and radii of curvature used are the nominal values for a 21.0D IOL as provided by the manufacturer and not the specific IOL thickness for the particular IOL power to be used). The second category is the *ACD Constant*. What makes this ACD constant

Table 36.12 Guide for changing the IOL constant with respect to the mean prediction error

Mean Prediction Error (D)	−0.50	−0.40	−0.30	−0.20	−0.10	0.00	+0.10	+0.20	+0.30	+0.40	+0.50
Hoffer Q pACD Holladay 1 sf Barrett UII Surgeon Factor Holladay 2 ACD Olsen ACD Haigis a0 (NOT a1, a2)	Decrease constant by 0.39	Decrease constant by 0.31	Decrease constant by 0.23	Decrease constant by 0.15	Decrease constant by 0.08	No Change of the IOL constant	Increase constant by 0.08	Increase constant by 0.15	Increase constant by 0.23	Increase constant by 0.31	Increase constant by 0.39
SRK/T A constant T2 A constant Kane A constant	Decrease constant by 0.625	Decrease constant by 0.500	Decrease constant by.375	Decrease constant by 0.250	Decrease constant by 0.125	No Change of the IOL constant	Increase constant by 0.125	Increase constant by 0.250	Increase constant by 0.375	Increase constant by 0.500	Increase constant by 0.625

different from other thin lens formulae is that the *ACD constant* is related to the physical IOL location. It is the average post-op ACD for a specific IOL model, derived from actual measurements of post-op AC, from the corneal epithelium to the anterior surface of the IOL, using a biometer.

To obtain an optimized Olsen ACD value, the surgeon selects a sufficiently large sample of eyes implanted with the same IOL model in the bag. For each eye, the **actual** post-op ACD is measured using optical biometry. Then, the surgeon calculates the average post-op ACD for the entire sample, and this value is entered as the ACD constant for this specific IOL model for the Olsen formula.

When the optimized Olsen ACD value is entered, the software for the Olsen formula then calculates the constant ***C***, which denotes the average anteroposterior position of the center of the IOL within the capsular bag after implantation.

$$\textbf{Predicted}\ \text{Postop ACD} = \text{Preop ACD} + \boldsymbol{C} * \left(\text{Lens Thickness}\right) - \frac{\text{IOL Thickness}}{2}$$

The surgeon does not need to perform any calculations to derive the C constant, all this is done by the software once the average post-op ACD is provided for a sample of eyes.

The geometry of the optic and haptics influences the anteroposterior location of the optic inside the capsular bag, so the C Constant varies from the IOL model to the IOL model in a similar way to other IOL constants, that is 1 mm of change corresponds to 1.4D of change in refraction at the spectacle plane. As the post-op ACD and the C constant are derived from physical data and not from an iterative process, there is a chance that the mean prediction error may not be 0 following optimization. This can be further refined to 0 using the empirical approach summarised in Table 36.12.

Another advantage of the Olsen formula is that one can use the physical location of the IOL for the first eye (by measuring the post-op ACD of that eye) to improve predictions for the second eye by replacing the predicted ACD value with the post-op ACD measured in the fellow eye [58], and this measurement should preferably be performed at least 1- month post-op [59].

C. The Naeser 1 and 2 formulae

The Naeser 1 formula is a thick lens vergence formula, which was first published in 1990 and 1997 [60, 61]. It predicts the post-op IOL position (in this case, the position of the post-op posterior lens capsule) using a double regression formula with respect to pre-op AL, pre-op ACD, and an intercept, similar to the Haigis formula, but in this case, the predicted position of the posterior lens capsule corresponds to the actual physical position and not a theoretical ELP.

Then, an optimized theoretical pre-op axial length value (the theoretical ideal pre-op AL to achieve 0 prediction error) is back calculated using another regression equation with an intercept and the actual pre-op AL with its coefficient. One establishes the value of the AL coefficient and the intercept based on the number of eyes. Once the intercept and the coefficient are determined, all future pre-op axial length measurements are converted to an optimized AL value using the optimized regression formula before entering that value in the equation.

For the first version of the formula (Naeser 1), one needs the actual physical dimensions (anterior and posterior radii for each IOL power and central IOL thickness) for each IOL power across the range of powers for that IOL model. This can be obtained using the manufacturer's cutting cards, but as this is proprietary information, they can be difficult to obtain. For the second version of the formula (Naeser 2) [62], these physical characteristics may be calculated with minimal loss of prediction accuracy.

D. The K6 Formula

This is a thin-lens general vergence formula with a single A-constant that was developed

using thick-lens techniques and then modified to work as a thin-lens formula. By measuring the post-op ACD in a number of eyes, one can solve the general vergence equation by back-calculating to find the total corneal power (K) using 6 variables (AL, Ks, ACD, CCT, LT, and HCD). The axial length is from a slightly modified CMAL (using slightly different refractive indices from what CMAL used) [63]. CMAL stands for Cooke's modified Axial Length, which corrects biases related to the proportion of the lens and vitreous optical path in short and long eyes as well as establishing the limit of the axial length at the RPE and not at the ILM as most formulas do. The K6 formula was developed with the Alcon IOL system. If a markedly different IOL platform is used, some internal adjustments to the formula need to be made, in addition to using a different A-constant (personal communication with the author).

E. The Castrop Formula

This formula uses a Gaussian thick lens formula for the cornea and a thin lens vergence formula for the IOL [64]. The ELP is derived from a regression equation containing the Axial Length (AL), the central corneal thickness (CCT), the Aqueous Depth (AQD), the Mean corneal radius (R_{mean}), and the Lens Thickness (LT).

$$\mathbf{ELP} = 0.61 + 0.049 * \mathrm{AL} + 0.000729 * \mathrm{CCT} + 0.680 * \mathrm{AQD} - 0.123 * R_{\mathrm{mean}} + \boldsymbol{C} * \mathrm{LT}$$

For eyes with a pathological cornea or previous refractive surgery, the ELP can be estimated by omitting the mean corneal radius and using the formula below. In post-refractive eyes, the IOL power calculation needs true corneal power measurements.

$$\mathbf{ELP} = -0.09 + 0.037 * \mathrm{AL} + 0.000602 * \mathrm{CCT} + 0.715 * \mathrm{AQD} + C * \mathrm{LT}$$

The original version of the formula contains two constants; one called *C*, which relates to the IOL model, and another called *R* used for offsetting other systematic errors derived from IOL optic asphericity or offsets related to the biometry method, etc. A new 3-constant version keeps the C constant as it is but divides the other constant into an "*H*" offset related to the biometry machine and an "*R*" related to refractive components (such as the amount of spherical aberration of the IOL), which cannot be dealt with Gaussian optics (personal communication with the author).

$$\mathbf{ELP} = 0.045 * \mathrm{AL} + 0.761 * \mathrm{ACD} - 0.042 * \overline{r}_{\mathrm{ant}} + \boldsymbol{C} * \mathrm{LT} + \boldsymbol{H}$$

The Castrop constants should be optimized using post-op refractions and iterative calculations.

Conclusions

When performing IOL power calculations, the optimized IOL constants used should be specific to (1) the model of the IOL to be implanted and (2) the biometry machine that was used. The starting values of these IOL constants should be provided by the biometry machine manufacturers via their representatives. Further optimizing the IOL constant for the individual surgeon is not expected to offer additional benefits for most surgeons' outcomes.

All cataract surgeons should audit their refractive outcomes to ensure that both their mean prediction error is 0 and their precision is within current standards. For the few surgeons who have an average prediction error significantly different from 0D, the IOL constant can be refined further to achieve a 0 mean prediction error. An important caveat to consider is that when using vision lanes shorter than 6 m for subjective refraction, the post-op refractive outcomes need adjusting to a far point of 6 m before they are used to guide IOL constant optimization.

The impact of using optimized IOL constants on refractive outcomes is often more significant compared to the small differences in outcomes between modern IOL power formulae.

Acknowledgments I thank Dr. Giacomo Savvini for providing the formula code for the Hoffer Q Holladay 1, SRK/T, and Haigis on MS Excel, Dr. Jaime Aramberri, and Dr. David Cooke for performing additional optimization calculations for unpublished IOL power formulae.

References

1. Aristodemou P, Knox Cartwright NE, Sparrow JM, Johnston RL. Intraocular lens formula constant optimization and partial coherence interferometry biometry: refractive outcomes in 8108 eyes after cataract surgery. J Cataract Refract Surg. 2011 Jan;37(1):50–62. https://doi.org/10.1016/j.jcrs.2010.07.037.
2. Dubey R, Birchall W, Grigg J. Improved refractive outcome for ciliary sulcus-implanted intraocular lenses. Ophthalmology. 2012 Feb;119(2):261–5. https://doi.org/10.1016/j.ophtha.2011.07.050.
3. Knox Cartwright NE, Aristodemou P, Sparrow JM, Johnston RL. Adjustment of intraocular lens power for sulcus implantation. JCRS. 2011;37(4):798–9.
4. Eom Y, Song JS, Kim HM. Modified Haigis formula effective lens position equation for ciliary sulcus-implanted intraocular lenses. Am J Ophthalmol. 2016 Jan;161:142–49.e1-2. https://doi.org/10.1016/j.ajo.2015.09.040.
5. Eom Y, Hwang HS, Hwang JY, Song JS, Kim HM. Posterior vault distance of ciliary sulcus-implanted three-piece intraocular lenses according to ciliary sulcus diameter. Am J Ophthalmol. 2017 Mar;175:52–9. https://doi.org/10.1016/j.ajo.2016.11.015.
6. Millar ER, Allen D, Steel DH. Effect of anterior capsulorhexis optic capture of a sulcus-fixated intraocular lens on refractive outcomes. J Cataract Refract Surg. 2013 Jun;39(6):841–4. https://doi.org/10.1016/j.jcrs.2012.12.034.
7. McMillin J, Wang L, Wang MY, Al-Mohtaseb Z, Khandelwal S, Weikert M, Hamill MB. Accuracy of intraocular lens calculation formulas for flanged intrascleral intraocular lens fixation with double-needle technique. J Cataract Refract Surg. 2020 Dec 9. https://doi.org/10.1097/j.jcrs.0000000000000540.
8. Randerson EL, Bogaard JD, Koenig LR, Hwang ES, Warren CC, Koenig SB. Clinical outcomes and lens constant optimization of the Zeiss CT Lucia 602 lens using a modified Yamane technique. Clin Ophthalmol. 2020 Nov 17;14:3903–12. https://doi.org/10.2147/OPTH.S281505.
9. Norrby S. Sources of error in intraocular lens power calculation. J Cataract Refract Surg. 2008 Mar;34(3):368–76. https://doi.org/10.1016/j.jcrs.2007.10.031.
10. Tehrani M, Krummenauer F, Kumar R, Dick HB. Comparison of biometric measurements using partial coherence interferometry and applanation ultrasound. J Cataract Refract Surg. 2003 Apr;29(4):747–52. https://doi.org/10.1016/s0886-3350(02)01739-x.
11. Haigis W, Lege B, Miller N, Schneider B. Comparison of immersion ultrasound biometry and partial coherence interferometry for intraocular lens calculation according to Haigis. Graefes Arch Clin Exp Ophthalmol. 2000 Sep;238(9):765–73. https://doi.org/10.1007/s004170000188.
12. Hoffer KJ, Shammas HJ, Savini G. Comparison of 2 laser instruments for measuring axial length. J Cataract Refract Surg. 2010 Apr;36(4):644–648. https://doi.org/10.1016/j.jcrs.2009.11.007. Erratum in: J Cataract Refract Surg. 2010 Jun;36(6):1066.
13. Rabsilber TM, Jepsen C, Auffarth GU, Holzer MP. Intraocular lens power calculation: clinical comparison of 2 optical biometry devices. J Cataract Refract Surg. 2010 Feb;36(2):230–4. https://doi.org/10.1016/j.jcrs.2009.09.016.
14. Huang J, Chen H, Li Y, Chen Z, Gao R, Yu J, Zhao Y, Lu W, McAlinden C, Wang Q. Comprehensive comparison of axial length measurement with three swept-source OCT-based biometers and partial coherence interferometry. J Refract Surg. 2019 Feb 1;35(2):115–20. https://doi.org/10.3928/1081597X-20190109-01.
15. Cooke DL, Cooke TL, Suheimat M, Atchison DA. Standardizing sum-of-segments axial length using refractive index models. Biomed Opt Express. 2020 Sep 25;11(10):5860–70. https://doi.org/10.1364/BOE.400471.
16. Kanclerz P, Hoffer KJ, Przewłócka K, Savini G. Comparison of the upgraded Revo NX with the IOLMaster 700 and the Lenstar. J Cataract Refract Surg 2020 Dec 14. https://doi.org/10.1097/j.jcrs.0000000000000541.
17. Li J, Chen H, Savini G, Lu W, Yu X, Bao F, Wang Q, Huang J. Measurement agreement between a new biometer based on partial coherence interferometry and a validated biometer based on optical low-coherence reflectometry. J Cataract Refract Surg. 2016 Jan;42(1):68–75. https://doi.org/10.1016/j.jcrs.2015.05.042.
18. Yang JY, Kim HK, Kim SS. Axial length measurements: comparison of a new swept-source optical coherence tomography-based biometer and partial coherence interferometry in myopia. J Cataract Refract Surg. 2017 Mar;43(3):328–32. https://doi.org/10.1016/j.jcrs.2016.12.023.
19. Yang CM, Lim DH, Kim HJ, Chung TY. Comparison of two swept-source optical coherence tomography biometers and a partial coherence interferometer. PLoS One. 2019 Oct 11;14(10):e0223114. https://doi.org/10.1371/journal.pone.0223114.
20. Tañá-Rivero P, Aguilar-Córcoles S, Tello-Elordi C, Pastor-Pascual F, Montés-Micó R. Agreement between two swept-source OCT biometers and a Scheimpflug partial coherence interferometer. J Cataract Refract Surg. 2020 Nov 23. https://doi.org/10.1097/j.jcrs.0000000000000483.

21. Oh R, Oh JY, Choi HJ, Kim MK, Yoon CH. Comparison of ocular biometric measurements in patients with cataract using three swept-source optical coherence tomography devices. BMC Ophthalmol. 2021 Jan 27;21(1):62. https://doi.org/10.1186/s12886-021-01826-5.
22. Fişuş AD, Hirnschall ND, Findl O. Comparison of two swept-source optical coherence tomography-based biometry devices. J Cataract Refract Surg. 2020 Aug 5. https://doi.org/10.1097/j.jcrs.0000000000000373.
23. Haddad JS, Barnwell E, Rocha KM, Ambrosio R Jr, Waring Iv GO. Comparison of biometry measurements using standard partial coherence interferometry versus new Scheimpflug tomography with integrated axial length capability. Clin Ophthalmol. 2020 Feb 4;14:353–8. https://doi.org/10.2147/OPTH.S238112.
24. Ortiz A, Galvis V, Tello A, Viaña V, Corrales MI, Ochoa M, Rodriguez CJ. Comparison of three optical biometers: IOLMaster 500, Lenstar LS 900 and Aladdin. Int Ophthalmol. 2019 Aug;39(8):1809–18. https://doi.org/10.1007/s10792-018-1006-z.
25. Huang J, McAlinden C, Huang Y, Wen D, Savini G, Tu R, Wang Q. Meta-analysis of optical low-coherence reflectometry versus partial coherence interferometry biometry. Sci Rep. 2017 Feb 24;7:43414. https://doi.org/10.1038/srep43414.
26. Shetty N, Kaweri L, Koshy A, Shetty R, Nuijts RMMA, Roy AS. Repeatability of biometry measured by IOLMaster 700, Lenstar LS 900 and Anterion, and its impact on predicted intraocular lens power. J Cataract Refract Surg. 2020 Nov 23. https://doi.org/10.1097/j.jcrs.0000000000000494.
27. Savini G, Taroni L, Schiano-Lomoriello D, Hoffer KJ. Repeatability of total Keratometry and standard Keratometry by the IOLMaster 700 and comparison to total corneal astigmatism by Scheimpflug imaging. Eye (Lond). 2021 Jan;35(1):307–15. https://doi.org/10.1038/s41433-020-01245-8.
28. Calvo-Sanz JA, Portero-Benito A, Arias-Puente A. Efficiency and measurements agreement between swept-source OCT and low-coherence interferometry biometry systems. Graefes Arch Clin Exp Ophthalmol. 2018 Mar;256(3):559–66. https://doi.org/10.1007/s00417-018-3909-9.
29. Pereira JMM, Neves A, Alfaiate P, Santos M, Aragão H, Sousa JC. Lenstar® LS 900 vs Pentacam®-AXL: comparative study of ocular biometric measurements and intraocular lens power calculation. Eur J Ophthalmol. 2018 Nov;28(6):645–51. https://doi.org/10.1177/1120672118771844.
30. Ruiz-Mesa R, Abengózar-Vela A, Ruiz-Santos M. Comparison of a new Scheimpflug imaging combined with partial coherence interferometry biometer and a low-coherence reflectometry biometer. J Cataract Refract Surg. 2017 Nov;43(11):1406–12. https://doi.org/10.1016/j.jcrs.2017.08.016.
31. Tu R, Yu J, Savini G, Ye J, Ning R, Xiong J, Chen S, Huang J. Agreement between two optical biometers based on large coherence length SS-OCT and Scheimpflug imaging/partial coherence interferometry. J Refract Surg. 2020 Jul 1;36(7):459–65. https://doi.org/10.3928/1081597X-20200420-02.
32. Srivannaboon S, Chirapapaisan C, Chonpimai P, Loket S. Clinical comparison of a new swept-source optical coherence tomography-based optical biometer and a time-domain optical coherence tomography-based optical biometer. J Cataract Refract Surg. 2015 Oct;41(10):2224–32. https://doi.org/10.1016/j.jcrs.2015.03.019.
33. Hoffer KJ, Hoffmann PC, Savini G. Comparison of a new optical biometer using swept-source optical coherence tomography and a biometer using optical low-coherence reflectometry. J Cataract Refract Surg. 2016 Aug;42(8):1165–72. https://doi.org/10.1016/j.jcrs.2016.07.013.
34. Cheng H, Li J, Cheng B, Wu M. Refractive predictability using two optical biometers and refraction types for intraocular lens power calculation in cataract surgery. Int Ophthalmol. 2020 Jul;40(7):1849–56. https://doi.org/10.1007/s10792-020-01355-y.
35. Rohrer K, Frueh BE, Wälti R, Clemetson IA, Tappeiner C, Goldblum D. Comparison and evaluation of ocular biometry using a new noncontact optical low-coherence reflectometer. Ophthalmology. 2009 Nov;116(11):2087–92. https://doi.org/10.1016/j.ophtha.2009.04.019.
36. Omoto MK, Torii H, Masui S, Ayaki M, Tsubota K, Negishi K. Ocular biometry and refractive outcomes using two swept-source optical coherence tomography-based biometers with segmental or equivalent refractive indices. Sci Rep. 2019 Apr 25;9(1):6557. https://doi.org/10.1038/s41598-019-42968-3. Erratum in: Sci Rep. 2020 Jul 31;10(1):13181.
37. Shammas HJ, Ortiz S, Shammas MC, Kim SH, Chong C. Biometry measurements using a new large-coherence-length swept-source optical coherence tomographer. J Cataract Refract Surg. 2016 Jan;42(1):50–61. https://doi.org/10.1016/j.jcrs.2015.07.042.
38. Huang J, Savini G, Li J, Lu W, Wu F, Wang J, Li Y, Feng Y, Wang Q. Evaluation of a new optical biometry device for measurements of ocular components and its comparison with IOLMaster. Br J Ophthalmol. 2014 Sep;98(9):1277–81. https://doi.org/10.1136/bjophthalmol-2014-305150.
39. Nemeth G, Modis L Jr. Ocular measurements of a swept-source biometer: repeatability data and comparison with an optical low-coherence interferometry biometer. J Cataract Refract Surg. 2019 Jun;45(6):789–97. https://doi.org/10.1016/j.jcrs.2018.12.018.
40. Mandal P, Berrow EJ, Naroo SA, Wolffsohn JS, Uthoff D, Holland D, Shah S. Validity and repeatability of the Aladdin ocular biometer. Br J Ophthalmol.

2014 Feb;98(2):256–8. https://doi.org/10.1136/bjophthalmol-2013-304002. Erratum in: Br J Ophthalmol. 2015 Dec;99(12):1746.
41. Reitblat O, Levy A, Kleinmann G, Assia EI. Accuracy of intraocular lens power calculation using three optical biometry measurement devices: the OA-2000, Lenstar-LS900 and IOLMaster-500. Eye (Lond). 2018 Jul;32(7):1244–52. https://doi.org/10.1038/s41433-018-0063-x.
42. Kongsap P. Comparison of a new optical biometer and a standard biometer in cataract patients. Eye Vis (Lond). 2016 Oct 17;3:27. https://doi.org/10.1186/s40662-016-0059-1.
43. Hua Y, Qiu W, Xiao Q, Wu Q. Precision (repeatability and reproducibility) of ocular parameters obtained by the Tomey OA-2000 biometer compared to the IOLMaster in healthy eyes. PLoS One. 2018 Feb 27;13(2):e0193023. https://doi.org/10.1371/journal.pone.0193023.
44. Haigis W. Matrix-optical representation of currently used intraocular lens power formulas. J Refract Surg. 2009 Feb;25(2):229–34. https://doi.org/10.3928/1081597X-20090201-09.
45. Holladay JT. Standardizing constants for ultrasonic biometry, keratometry, and intraocular lens power calculations. J Cataract Refract Surg. 1997 Nov;23(9):1356–70. https://doi.org/10.1016/s0886-3350(97)80115-0.
46. Bucher PJ. Anterior chamber depth with sulcus and capsular bag placed IOGEL lenses. J Cataract Refract Surg. 1990 Nov;16(6):737–40. https://doi.org/10.1016/s0886-3350(13)81017-6.
47. Gimbel HV. Evolving techniques of cataract surgery: continuous curvilinear Capsulorhexis, down-slope sculpting, and nucleofractis. Semin Ophthalmol. 1992 Dec;7(4):193–207. https://doi.org/10.3109/08820539209065108.
48. Armstrong TA. Refractive effect of capsular bag lens placement with the capsulorhexis technique. J Cataract Refract Surg. 1992 Mar;18(2):121–4. https://doi.org/10.1016/s0886-3350(13)80916-9.
49. Hughes RA, Aristodemou P, Sparrow JM, Kaye S. Multilevel multivariate modelling of the effect of gender and patient co-morbidity on spherocylindrical refractive outcome following cataract surgery – submitted for publication late 2020 – scientific reports.
50. Simpson MJ, Charman WN. The effect of testing distance on intraocular lens power calculation. J Refract Surg. 2014 Nov;30(11):726. https://doi.org/10.3928/1081597X-20141021-01.
51. Hoffer KJ. The Hoffer Q formula: A comparison of theoretic and regression formulas. J Cataract Refract Surg. 1993;19(11):700–12. Errata: 1994;20(6):677 and 2007;33(1):2–3
52. Holladay JT, Prager TC, Chandler TY, Musgrove KH, Lewis JW, Ruiz RS. A three-part system for refining intraocular lens power calculations. J Cataract Refract Surg. 1988 Jan;14(1):17–24. https://doi.org/10.1016/s0886-3350(88)80059-2.
53. Retzlaff JA, Sanders DR, Kraff MC. Development of the SRK/T intraocular lens implant power calculation formula. J Cataract Refract Surg. 1990;16:333–40. Errata: 1990;16:528 and 1993;19(5):444–446
54. Hoffer KJ. Errata in printed Hoffer Q formula. J Cataract Refract Surg. 2007;33:2–3.
55. Retzlaff JA, Sanders DR, Kraff MC. Erratum in. J Cataract Refract Surg. 1990 Jul;16(4):528.
56. Cooke DL, Cooke TL. Effect of altering lens constants. J Cataract Refract Surg. 2017 Jun;43(6):853. https://doi.org/10.1016/j.jcrs.2017.05.001.
57. Olsen T. Calculation of intraocular lens power: a review. Acta Ophthalmol Scand. 2007 Aug;85(5):472–85. https://doi.org/10.1111/j.1600-0420.2007.00879.x.
58. Olsen T. Use of fellow eye data in the calculation of intraocular lens power for the second eye. Ophthalmology. 2011 Sep;118(9):1710–5. https://doi.org/10.1016/j.ophtha.2011.04.030.
59. Muthappan V, Paskowitz D, Kazimierczak A, Jun AS, Ladas J, Kuo IC. Measurement and use of postoperative anterior chamber depth of fellow eye in refractive outcomes. J Cataract Refract Surg. 2015 Apr;41(4):778–84. https://doi.org/10.1016/j.jcrs.2014.08.034.
60. Naeser K, Boberg-Ans J, Bargum R. Biometry of the posterior lens capsule: a new method to predict pseudophakic anterior chamber depth. J Cataract Refract Surg. 1990 Mar;16(2):202–6. https://doi.org/10.1016/s0886-3350(13)80731-6.
61. Naeser K. Intraocular lens power formula based on vergence calculation and lens design. J Cataract Refract Surg. 1997 Oct;23(8):1200–7. https://doi.org/10.1016/s0886-3350(97)80316-1.
62. Næser K, Savini G. Accuracy of thick-lens intraocular lens power calculation based on cutting-card or calculated data for lens architecture. J Cataract Refract Surg. 2019 Oct;45(10):1422–9. https://doi.org/10.1016/j.jcrs.2019.05.021.
63. Cooke DL, Cooke TL. Approximating sum-of-segments axial length from a traditional optical low-coherence reflectometry measurement. J Cataract Refract Surg. 2019 Mar;45(3):351–4. https://doi.org/10.1016/j.jcrs.2018.12.026.
64. Wendelstein J, Hoffmann P, Hirnschall N, Fischinger IR, Mariacher S, Wingert T, Langenbucher A, Bolz M. Project hyperopic power prediction: accuracy of 13 different concepts for intraocular lens calculation in short eyes. Br J Ophthalmol. 2021 Jan 27. https://doi.org/10.1136/bjophthalmol-2020-318272.